Journal of Physics:
Conference Series

OPEN ACCESS

Damping of materials and members in structures

To cite this article: F Orban 2011 *J. Phys.: Conf. Ser.* **268** 012022

View the article online for updates and enhancements.

You may also like

- Characterization of energy dissipative cushions made of Ni–Ti shape memory alloy
Ahmet Güllü, Josiah Owusu Danquah and Sava Dilibal
- A geometric theory of selective decay with applications in MHD
François Gay-Balmaz and Darryl D Holm
- Experimental characterization of superelastic friction dampers with a focus on cyclic response, failure behavior and reparability
Malik Corum, Liang Cao, Fei Shi et al.

Enabling Electrochemistry
Inside and Outside the Lab

PalmSens

Discover our diverse range of Potentiostats engineered to support your research wherever it takes you

- Intuitive software for Windows and Android
- Proven in over 4000 scientific publications
- Single-channel and multi-channel
- Benchtop, portable and wearable

Discover More



This content was downloaded from IP address 216.73.216.56 on 19/11/2026 at 09:00

Journal of Physics: Conference Series **268** (2011) 012022 doi:10.1088/1742-6596/268/1/012022

Damping of materials and members in structures

F Orban

Department of Mechanical Design. Pollack Mihaly Faculty of Engineering
University of Pécs, Pécs, Hungary

E-mail: orb@witch.pmmf.hu

Abstract. The state of a structure subject to oscillatory deformation can be described by the combination of kinetic and potential energy. In the case of real structures there is also an energy dissipative element as some of the energy is lost per deformation cycle. The energy dissipation is caused by material damping which basically depends on three factors: amplitude of stress, number of cycles and geometry. In the case of non-homogeneous stress distribution the geometry of the structure influences the vibration damping. In this paper the influence of the geometry will be investigated with special regard to the cross-section. The examinations can be executed experimentally, theoretically and by the help of computer programs using FEM. In most cases the main goal is to increase the damping of the structure.

1. Measures of damping

Damping of structures is a very complex phenomenon, which refers to two basic reasons a) material damping b) friction damping at the connections. When a structure is subject to oscillatory deformations the state of the structure can be described by the combination of kinetic and potential energy. In the case of real structures some of this energy is lost per deformation cycles and this is called material damping.

Damping is the conversion of mechanical energy of a vibrating structure into thermal energy. If we want to quantify the level of damping in a structure the absorbed energy per cycle must be determined. By plotting the force versus displacement for a given cycle of motion a hysteresis curve is generated (figure 1).

At linear damping the hysteresis loop is an ellipses (figure 1a). In general metals have linear damping in the case when the stress amplitude less than the fatigue limit. At nonlinear damping the hysteresis loop is peaked when damping is a result of friction (figure 1b) One possibility to quantify the level of damping is to determine the area captured within the hysteresis loop

$$D = \oint F \cdot dy \,, \tag{1}$$

then the specific damping coefficient is:

$$\psi = \frac{D}{U} \,, \tag{2}$$

where U is the stored energy during loading.
For an unforced damped single degree of freedom (SDOF) system the general equation of motion becomes:

Published under licence by IOP Publishing Ltd

$$m \cdot \ddot{y} + k \cdot \dot{y} + \frac{y}{c} = 0\,, \tag{3}$$

where m is the mass, k is viscous damping constant and c is the spring constant.

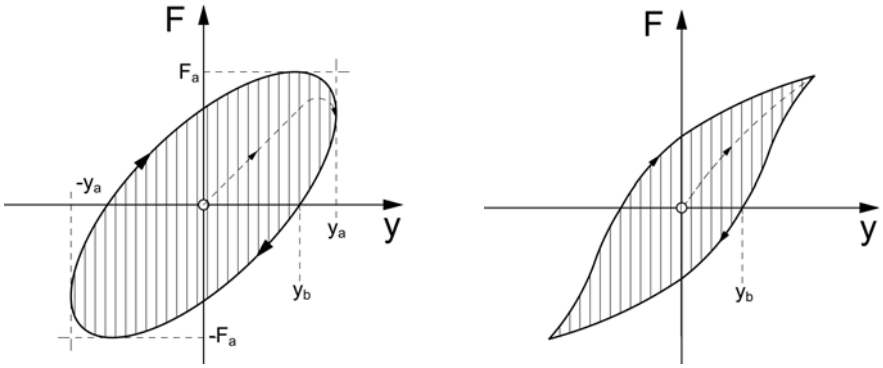


Figure 1. Hysteresis loop a) linear damping b) non linear damping.

In the under-damped case when $\beta < \alpha$

$$\alpha^2 = \frac{1}{m \cdot c}; \qquad \beta = \frac{k}{2m}\,, \tag{4}$$

$$\ddot{y} + 2\beta \cdot \dot{y} + \alpha^2 \cdot y = 0\,. \tag{5}$$

The solution is given by.

$$y(t) = A \cdot \mathrm{e}^{-\beta t} \cdot \sin(\gamma t + \varepsilon_0)\,, \tag{6}$$

where

$$\gamma = \sqrt{\alpha^2 - \beta^2}\,, \tag{7}$$

$$\frac{A_1}{A_2} = \frac{\mathrm{e}^{-\beta T}}{\mathrm{e}^{-\beta(t+T)}} = \mathrm{e}^{\beta T}\,, \tag{8}$$

$$\delta = \ln\frac{A_1}{A_2} = \frac{1}{k}\ln\frac{A_i}{A_{i+k}}\,. \tag{9}$$

The log decrement of transient response δ at linear damping is irrespective of time. There is a simple interrelationship between the specific damping coefficient ψ and the log decrement of transient response δ. It is possible to express the variable ψ as

$$\Psi = -\int_{U_i}^{U_{i+T}} \frac{dU}{U} = \ln\frac{U_i}{U_{i+T}}\,. \tag{10}$$

The potential energy for a spring is

$$U = \frac{y^2}{2c}\,, \tag{11}$$

$$\psi = \ln\frac{U_i}{U_{i+T}} = \ln\frac{A_i^2}{A_{i+T}^2} = 2\ln\frac{A_i}{A_{i+T}} = 2\delta\,. \tag{12}$$

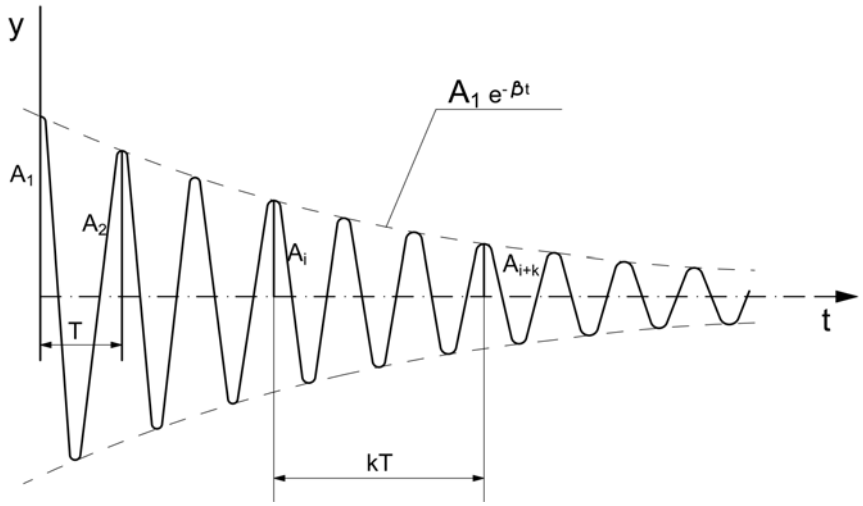


Figure 2. Transient response of a classically under-damped system.

The level of damping can be subjectively determined by noting the sharpness of resonant peak at f_1 (figure 3). For a quantitative measure of damping the Half-Power Bandwidth Method can be employed.

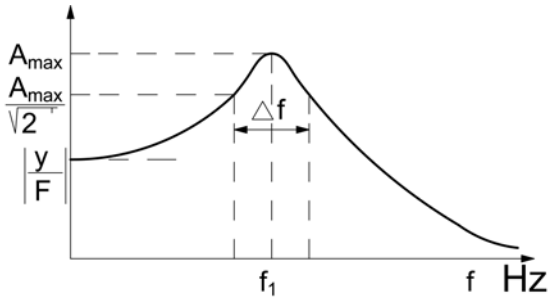


Figure 3. Compliance transfer function for a SDOF system.

The damping of the structure η can be determined from the ratio Δf to f_1. The resonant peak value is A_{max} and in this case the loss factor can be expressed as

$$\eta = \frac{\Delta f}{f_1}\,. \tag{13}$$

2. Material damping

Material damping depends on many factors. The most important of these factors are: type of materials, stress amplitude, internal forces, the number of cycles, sizes of geometry, the quality of surfaces and temperature. The factors were examined in Lazan book [1]. Damping depends mainly on the stress amplitude as

$$D = J \cdot \sigma_a^n\,, \tag{14}$$

where J and n are constants.

The value of n can be between 2 and 4 but generally $n = 2.3$ is used. Damping increases with the number of cycles and finally a fatigue collapse happens. The values of J are very different for the same material according different authors.

According to [2] $J = 2.326 \cdot 10^{-8}$ for low carbon steel and therefore

$$D = 2.321 \cdot 10^{-8} \cdot \sigma^{2.3} . \tag{15}$$

At the uniaxial stressed state the stored energy can be calculated:

$$U = \frac{\sigma^2}{2 \cdot E}, \tag{16}$$

$$\psi = \frac{D}{U} = 9.769 \cdot 10^{-3} \cdot \sigma^{0.3} . \tag{17}$$

According to Equation (17) the values computed for ψ are summarised in table 1.

Table 1. Specific damping coefficient values refers to σ_{MAX}.

σ N/mm^2	20	40	60	80	100	120	140
ψ %	2.4	2.9	3.3	3.7	3.9	4.1	4.3

The relationship between measures of damping can be expressed:

$$\eta = \frac{\psi}{2\pi} = \frac{\delta}{\pi} = 2\,\xi \ . \tag{18}$$

The values of the viscous damping ratio ξ is listed in table 2 according to [3].

Table 2. Dynamic properties of materials under standard conditions.

Representative Damping Ratios	
System	Viscous Damping Ratio ξ
Metals (in elastic range)	< 0.01
Continuous Metal Structures	0.02 to 0.04
Metal Structure with Joints	0.03 to 0.07
Aluminium / Steel Transmission Lines	≈ 0.0004
Small Diameter Piping Systems	0.01 to 0.02
Large Diameter Piping Systems	0.02 to 0.03
Auto Shock Absorbers	≈ 0.30
Rubber	≈ 0.05
Large Buildings during Earthquakes	0.01 to 0.05

3. Material damping in the structure

If the stress distribution is not homogeneous, the geometry of the structure influences the damping properties. The damping, which belongs to the maximum stress amplitude is

$$D_{am} = J \cdot \sigma_{am} . \tag{19}$$

The structural damping can be calculated as

$$D_s = D_{am} \cdot V \cdot \alpha_k \cdot \alpha_h , \tag{20}$$

where V is the volume of the structure, α_k is the cross section factor, α_h is the length factor.

The cross section factor for a rectangular cross section (figure 4a) is

$$\alpha_k = \frac{1}{A_0 \cdot y^n{}_{\max}} \cdot 2 \int_{y=0}^{b/2} a \cdot y^n \cdot dy = \frac{1}{n+1} , \tag{21}$$

where $A_0 = a \cdot b$.

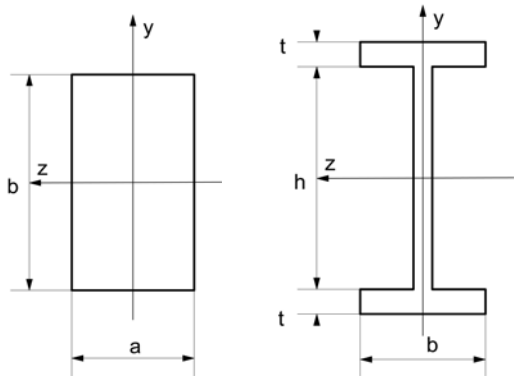


Figure 4. a) rectangular, b) I-section.

In the case of an I-section the cross section factor is:

$$\alpha_k = \frac{2}{A_0 \left(\frac{h}{2}\right)^n} \left[t_w \int_0^{h/2} y^n \cdot dy + b \cdot t \cdot \left(\frac{n}{2}\right)^n \right] = 1 - \frac{n}{n+1} \cdot \frac{t_w \cdot h}{A_0} . \tag{22}$$

It can be seen that the cross-section factor for an I-section is twice as big as for the rectangular section. The length factor is calculated as

$$\alpha_h = \frac{1}{l} \int_0^l \left(\frac{\sigma_{ax}}{\sigma_{am}} \right)^n dx . \tag{23}$$

A cantilever beam with concentrated load is plotted in figure 5. If the load is concentrated on the cantilever beam then the length factor is

$$\alpha_h = \frac{1}{l} \int_0^l \left(\frac{x}{l} \right)^n dx = \frac{1}{n+1} . \tag{24}$$

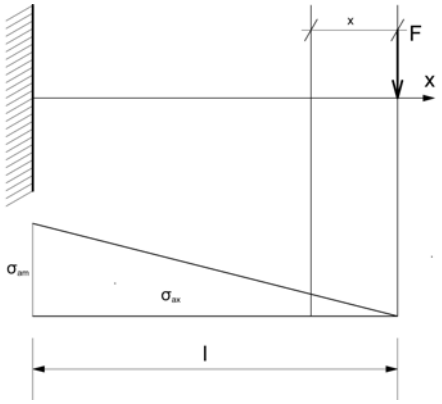


Figure 5. Maximum stress distribution at cantilever beam.

A cantilever beam with distributed load can be seen in figure 6.

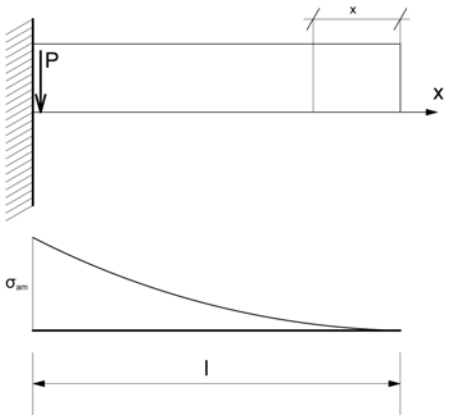


Figure 6. Maximum stress distribution at cantilever beam.

If the load is distributed load the length factor is

$$\alpha_h = \frac{1}{l}\int\left(\frac{x^2}{l^2}\right)^n dx = \frac{1}{2n+1}. \tag{25}$$

A simply supported beam with concentrated load is plotted in figure 7.

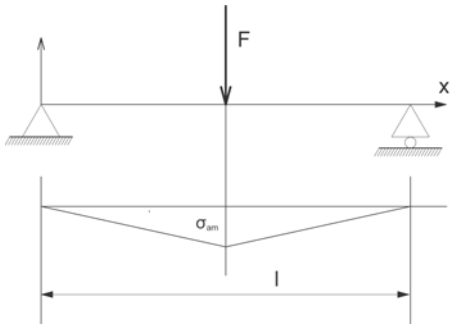


Figure 7. Maximum stress distribution at simply supported beam.

If the load is concentrated the length factor for a simple beam can be determined as

$$\alpha_h = \frac{1}{l} 2 \int_0^{l/2} \left(\frac{2x}{l} \right)^n dx = \frac{1}{n+1}. \tag{26}$$

Simply supported beam with concentrated load is plotted in figure 8.

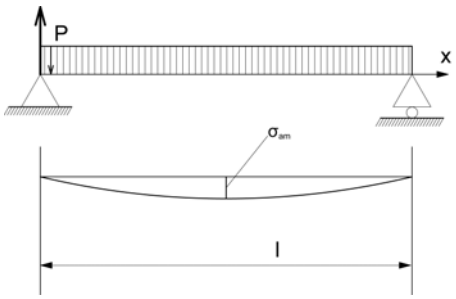


Figure 8. Maximum stress distribution at simply supported beam.

In this case the length factor can be determined as

$$\alpha_h = \frac{1}{l} \int_0^l \left[\frac{4}{l^2} \left(l_x - x^2 \right) \right]^n dx = \frac{2}{3} \left(\frac{3}{4} \right)^n + \frac{1}{6}. \tag{27}$$

4. Damping analysis with FEM

The effect of the geometry on the damping will be analyzed by finite element method (FEM) in this section. The GEOSTAR program controls the complete operations of the COSMOSM package and all modules are accessed from there.

The FREQUENCY/BUCKLING option of the program calculates the frequencies without damping The POST DYNAMIC analysis (ASTAR) is used to examine the damping and for this it is necessary to define the damping ratio ξ. Load excitations may be applied as concentrated loads at specified nodes or as distributed pressure applied to specified element faces. The response of the structure at certain nodes may be calculated for displacement.

The log decrement of a transient response is calculated with the help of the displacement time curve.

$$\delta = \frac{1}{k} \ln \frac{A_i}{A_{i+k}}, \tag{28}$$

$$\delta = \beta \cdot T, \tag{29}$$

$$\beta = \frac{\delta}{T} = 2\pi\xi \cdot f_1. \tag{30}$$

The calculated values β and T are suitable for measuring damping. The force-time diagram shown in figure 9 will applied as an excitation. The examined cross-sections can be seen in figure 10.

Six models were examined according to table 3.

In the examined cases the cross-section area were the same and the maximum stresses were the same for a given beam, in the case of the cantilever beam 75 MPa and for the simply supported beam 20 MPa.

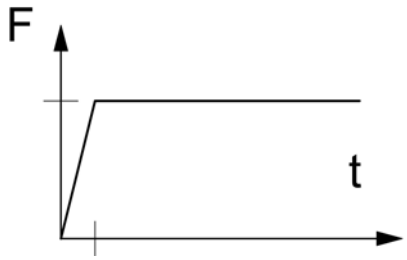


Figure 9. Force-time diagram.

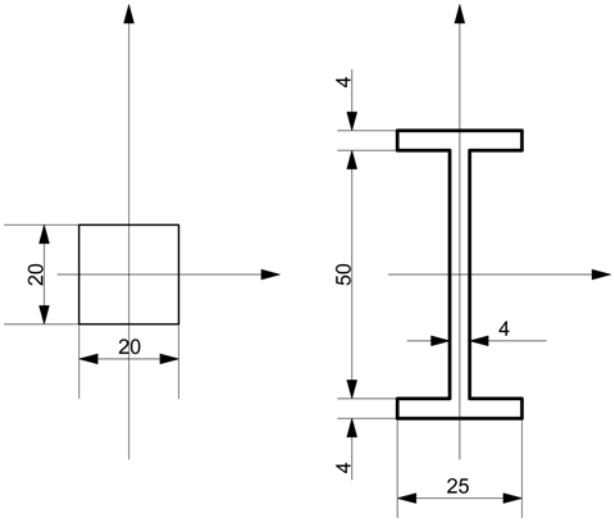


Figure 10. Dimensions of the cross-section.

Table 3. The investigated models

Model	Type of beam	Loading	Cross-section	Max stress
1.	cantilever	Force end of the beam	□	75 MPa
2.	cantilever	Force end of the beam	I	75 MPa
3.	cantilever	distributed load	□	75 MPa
4.	simply supported	distributed load	□	20 MPa
5.	simply supported	distributed load	I	20 MPa
6.	simply supported	Force end of the beam	I	20 MPa

Computation of the damping is illustrated in figure 11, where the beam is fixed and the cross-section is rectangular.

The damping results for a fixed beam with an I-section can be seen in figure 12.

The results are listed in table 4.

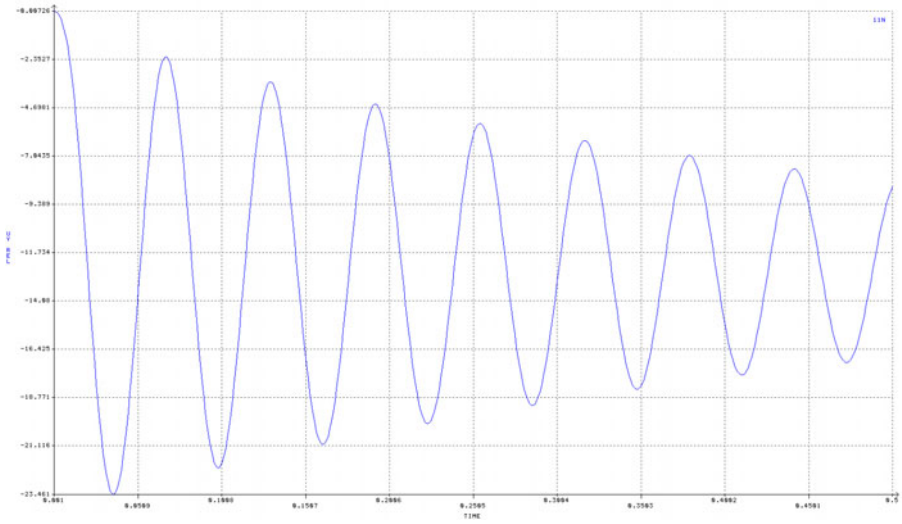


Figure 11. Damped vibration for a fixed beam with rectangular cross-section.

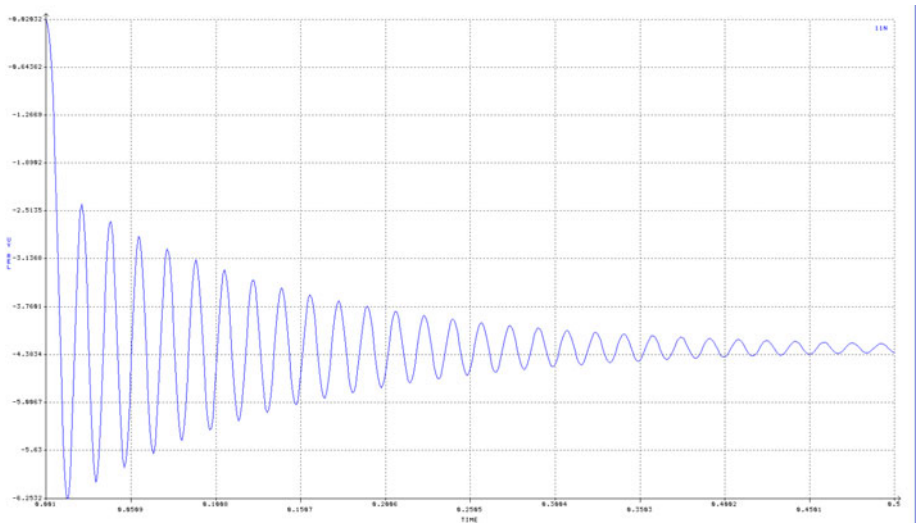


Figure 12. Damped vibration for a fixed beam with an I-section.

Table 4. Calculated results for β eigenvalue frequency.

Model	β	f_1 [H_z]
1.	2.08	16.06
2.	4.05	60.2
3.	1.77	16.06
4.	5.78	45.3
5.	20.67	170
6.	17.36	170

The cross section factor α_k for I section (figure 4b) is twice as high as for the rectangular section (figure 4a). According to the FEM calculations the results are similar. The effects of the load distribution are smaller.

5. Measuring the damping in a laboratory

Different methods exist to measure the characteristics of damping. In one method the starting displacement is applied and then the system is left free to move (figure 13). In this case a damped vibration can be observed. To determine the changing of amplitudes the log decrement δ can be calculated, however the changing of amplitudes and strain changing near the fixed point is the same. Strain-gauge was used to measure the strains. Figure 14 illustrates the acceleration of beam end and strain changing. From the measured values the value of β can be calculated. The first 10 amplitudes according to measurements are listed in table 5.



Figure 13. Arrangement of measurement.

Table 5. Measurement results.

Strain (μ/m)	Time (s)	Acceleration m s^{-2}
355.68	0.44	-.0.72
307.44	0.54	-0.1
269.04	0.64	-0.089
220.08	0.74	-0.074
268.8	0.85	-0.086
232.08	0.95	-0.075
240.96	1.07	-0.075
250.56	1.17	-0.078
247.92	127	-0.078
233.76	1.37	-0.074

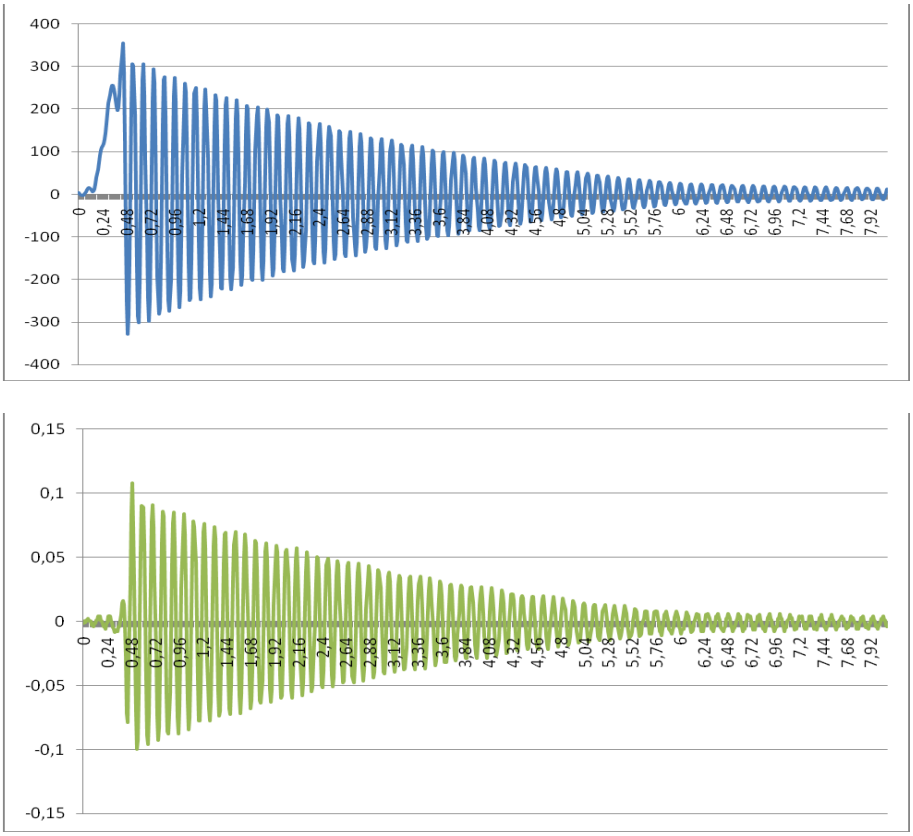


Figure 14. Acceleration of the beam end and strains changing near the fixed point

The model of the experiment can be seen in figure 15. The parameters for the model are l =550 mm, a= 10 mm, m_{beam} = 0.434 kg, m = 0.5 kg.

$$E = 2.1 \cdot 10^5 \,\mathrm{MP}, \quad c = \frac{l^3}{3IE}, \tag{31}$$

$$\alpha = \sqrt{\frac{1}{m_{red} \cdot c}}. \tag{32}$$

The eigenvalue frequency is

$$f = \frac{\alpha}{2\pi} = 10.55 \,\mathrm{Hz}, \qquad T = 0.094 \,s, \tag{33}$$

$$\delta = \frac{1}{k} \ln \frac{A_1}{A_{10}} = \frac{1}{9} \ln \frac{355.86}{233.76} = 0.04669 \tag{34}$$

and the results of the measurements:

$$T = \frac{1.37 - 0.44}{9} = 0.103 \,\mathrm{sec}, \tag{35}$$

$$f = \frac{1}{T} = 9.708 \,\mathrm{Hz}. \tag{36}$$

The calculated and measured values are very close to each other. In this case the damping ratio becomes:

$$\xi = \frac{\delta \cdot f}{\alpha} = 0.007 . \tag{37}$$

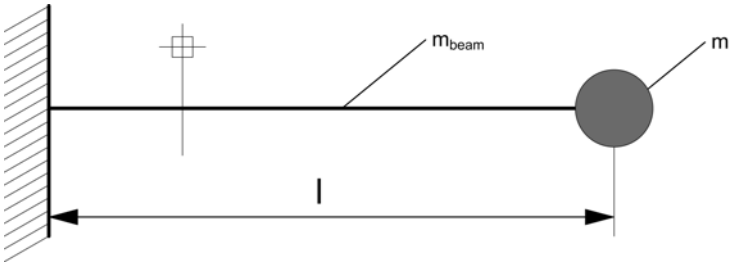


Figure 15. The model of the experiment.

6. Calculating structural damping

Let us determine the structural damping for the model shown in figure16.

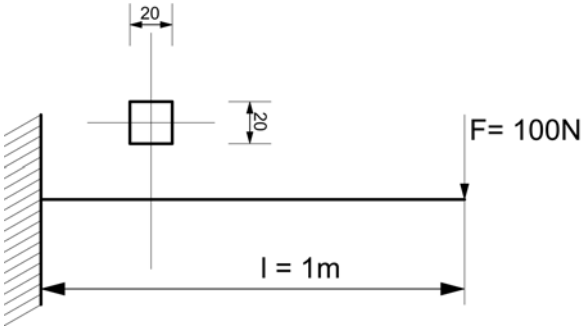


Figure 16. Dimensions of the cantilever beam.

$$\sigma_{MAX} = \frac{M_{MAX}}{W} = \frac{100}{1.333} = 75 \text{ N/mm}^2 . \tag{38}$$

The maximum displacement at the end of the beam is:

$$y_{MAX} = \frac{F \cdot l^3}{3IE} = \frac{100 \cdot 1000^3}{3 \cdot 1.333 \cdot 10^4 \cdot 2.1 \cdot 10^5} = 12.5 \text{ mm} . \tag{39}$$

The damping ratio according to the measurements is ξ =0.007. The loss factor is η = 0.014, the log decrement is δ = 0.044 and the absorbed energy is

$$U = W = \frac{1}{2} F \cdot y_{MAX} = 625 \text{ N mm} . \tag{40}$$

The structural damping result is

$$D_s = \psi \cdot U = 2\delta \cdot U = 55 \text{ N mm} . \tag{41}$$

The damping of the structure can be increased by using sandwich beams.

7. Sandwich beams

Comparing the damping properties of this model the dimensions of this beam are selected according to figure 17.

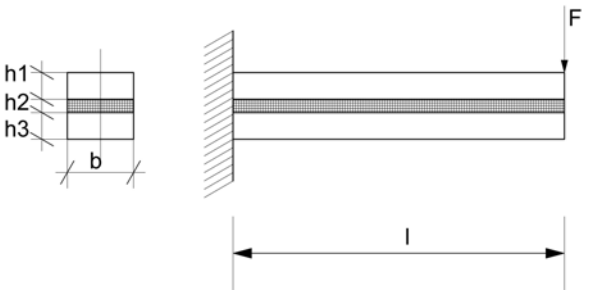


Figure 17. Sandwich beam.

Calculation of the maximum stress data is shown in figure 18.

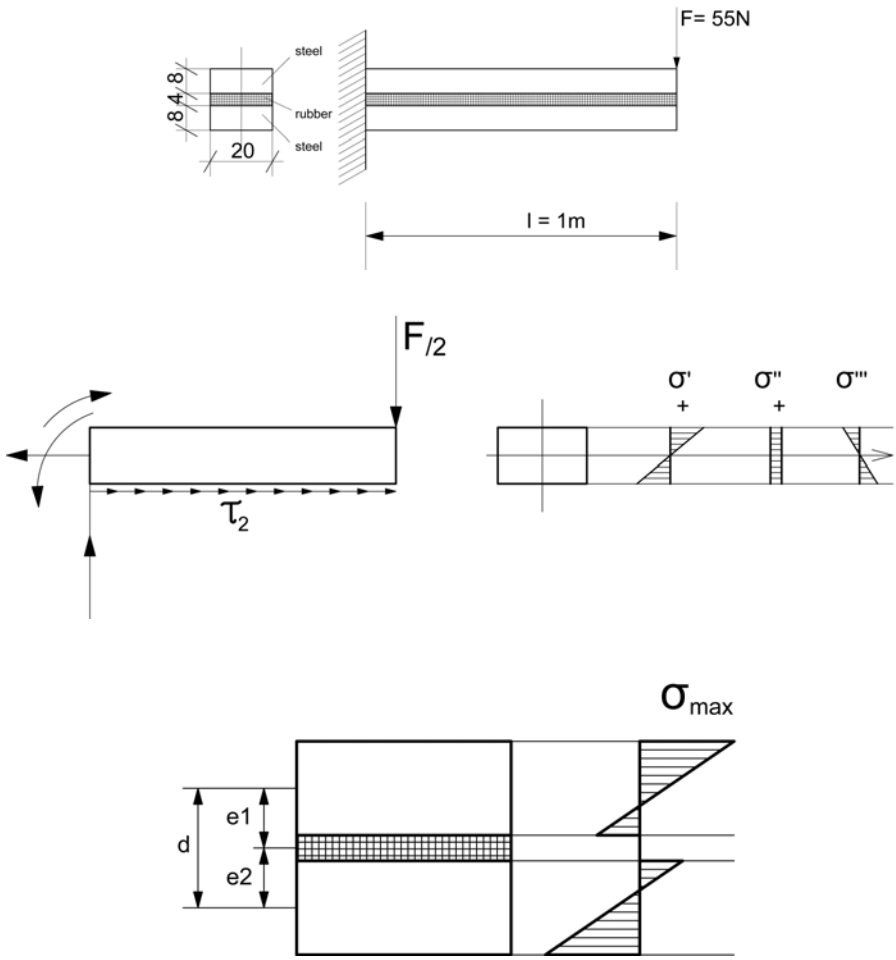


Figure 18. Stress distribution of the sandwich beam.

To calculate the normal stresses the following expressions are applied:

$$\sigma' = \frac{F \cdot l}{2W_1}, \quad \sigma'' = \frac{\tau_2 \cdot b \cdot l}{2A_1}, \quad \sigma''' = \frac{\tau_2 \cdot b \cdot l \cdot h_1}{4W_1}, \tag{42}$$

$$\sigma_{MAX} = 128.9 + 24.75 - 74.25 = 79.4 \text{ N/mm}. \tag{43}$$

The maximum displacement at the end of beam is

$$y_{MAX} = 19.52 \text{ mm}.$$

The loss factor can be calculated using the formula for sandwich beams developed by Ungar [4] (also in Farkas [5])

$$\eta = \frac{\eta_2 \cdot XY}{1 + (2 + Y) + (1 + Y)(1 + \eta_2^2) \cdot X^2}, \tag{44}$$

where η_2 is the loss factor of the rubber, X is the shear parameter and Y is the stiffness parameter of the laminates.

$$X = g_0 \left(\frac{C_d \cdot L}{2\pi} \right), \tag{45}$$

$$g_0 = \frac{2G_d \cdot b}{h_2 \sum A_i E_i}, \tag{46}$$

$$Y = \frac{d^2 \cdot b}{B_f} \cdot \frac{E_1 \cdot h_1 \cdot E_3 \cdot h_3}{E_1 \cdot h_1 + E_3 \cdot h_3}. \tag{47}$$

For steel $E_1 = E_2 = 2.1 \cdot 10^5$ MPa , for rubber G_d = 4.5 MPa and η_2 = 1.8, thus the loss factor of a sandwich beam is η= 0.0738. The calculated absorbed energy is

$$U = W = \frac{1}{2} F \cdot y_{MAX} = 536.8 \text{ N mm}, \tag{48}$$

$$\psi = 2\pi \cdot \eta = 0.4637. \tag{49}$$

The structural damping of a sandwich beam is:

$$D_s = \psi \cdot U = 248.9 \text{ N mm}. \tag{50}$$

The dissipative energy is more than four times higher then it is in the steel beam case, which has similar dimensions.

8. Other structures

Damping of different structures can be investigated similarly to the beams, however it is impossible to determine the damping of a structure theoretically. A possible way to compare different structures and determine which structure has better damping ability is to determine the value of β or T.

Figure 19 shows the first vibration mode shape in the case of the square plate stiffened by flat ribs. The cover plate is simply supported around the contour.

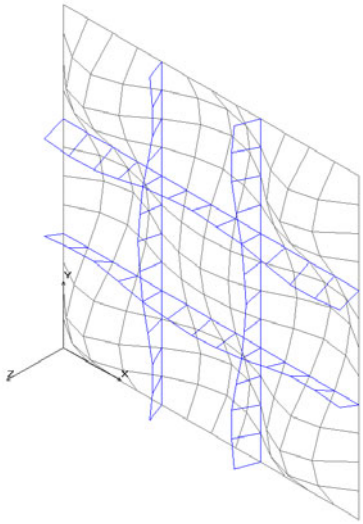


Figure 19. The first vibration mode shape at stiffened plates.

The calculation has been evaluated by FEM. The first natural frequency is f_1 = 49.27 Hz and the time of period is T_1 = 0.02 sec. Dimensions of the stiffened plates are: cover plate is 1410x1410x2 mm; flat ribs are 1410x90x3 mm. To examine a flat plate the dimensions are 1410x1410x2.5 mm, the first natural frequency is f_1 = 6.17 Hz and the time of period is T_1 = 0.16 sec. The examined two structures have the same volume. The stiffened plate has better damping ability according expression (30).

References

[1] Lazan B J 1968 *Damping of materials and members in structural mechanics* (Oxford Pergamon Press Oxford)
[2] Ponomarjov S D 1966 *Static design of mechanical structures* (in Hungarian) (Műszaki Könyvkiaidó Budapest)
[3] Cremer L and Heckl M 1988 *Structure borne sound* (Springer Verlag New York)
[4] Ungar E E 1962 Loss factors of visco-elastically damped beam structures *J Acoust. Soc. Amer* **18** 1082
[5] Farkas J 1984 *Optimum design of metal structures* (Budapest. Akadémiai Kiadó Chichester: Ellis Horwood)